Dopant Emission Mechanism and the Effects of Host Materials on the Behavior of Doped Organic Light-Emitting Diodes

Chengfeng Qiu, Haiying Chen, Man Wong, *Senior Member, IEEE*, and Hoi S. Kwok

***Abstract*—Organic light-emitting diodes made of tris-8-(hydroxyquinoline) aluminum as the electron-transport layers, N, N′-diphenyl-N, N′ bis (3-methylphenyl)-1, 1′-biphenyl-4,4′-diamine (TPD) as the hole-transport layers, and 2-(1, 1-dimethylethyl)-6(2-(2, 3, 6, 7-tetrahydro-1, 1, 7, 7-tetramethyl-1H, 5H-benzo(ij) quinolizin-9-yl) ethenyl)-4H-pyran-4-ylidene) propanedinitrile (DCJTB) as the guest dopant have been studied. It is determined that a) emission from guest DCJTB in a host transport material results primarily from separate trapping of holes and electrons, rather than the more commonly proposed Förster transfer mechanism, b) DCJTB is a more efficient hole than electron trap, and c) the lifetime of a doped device is longer when TPD is used as the host material.**

***Index Terms*—Carrier trapping, doping, emission mechanism, lifetime, organic light-emitting diode.**

I. Introduction

BECAUSE of their all solid-state nature, high brightness, low power consumption, capability of emitting a wide range of colors and ease of processing, organic light-emitting diodes (OLEDs) have been intensely studied [1]–[3] since the demonstration of efficient electroluminescence (EL) from a bilayer device by Tang *et al.* [4]. For realizing practical full-color displays, red-, green-, and blue-emitters with sufficiently high luminous efficiencies and color purity are required. Two common methods of tuning the color of an OLED are a) choosing an emission material with the appropriate intrinsic emission characteristics [5], [6] or b) incorporating in a host transport material guest dopants with the appropriate emission characteristics [7], [8].

Exciton formation in a guest dopant molecule could result from either the transfer (Förster or Dexter [5]) of an exciton formed in the host to the guest molecule or the sequential trapping of a hole and an electron [9] (not necessarily in this order) by the guest molecule. In the latter mechanism, the molecule becomes charged upon the capture of a first charge carrier. The resulting strong Coulomb interaction greatly increases the capture cross section of a second carrier of the opposite polarity. In organic small-molecule devices, the incorporation of certain kinds of guest dopants in the hole-transport layer (HTL) [10], [11], the electron-transport layer (ETL) [12], [13], or the anode buffer layer [14] has been reported to significantly enhance device luminous efficiencies and operating lifetimes.

In this work, the behavior of doped OLEDs based on tris-8-(hydroxyquinoline) aluminum (Alq_3) as the ETL and N, N′-diphenyl-N, N′ bis (3-methylphenyl)-1, 1′-biphenyl-4, 4′-diamine (TPD) as the HTL has been investigated. A red emission dopant, 2-(1, 1-dimethylethyl)-6(2-(2, 3, 6, 7-tetrahydro-1, 1, 7, 7-tetramethyl-1H, 5H-benzo(ij) quinolizin-9-yl) ethenyl)-4H-pyran-4-ylidene) propanedinitrile (DCJTB), has been used. It can be argued, by studying the effects of different placements of the dopant molecules, that sequential trapping rather than Förster exciton transfer [15] is the most likely dopant emission mechanism. Similar arguments have been made when 5, 6, 11, 12-tetraphenylnapthacene (rubrene) was used as the emission dopant in the TPD/Alq_3 system [16].

While shorter than the lifetime of an OLED without DCJTB, the lifetime of an OLED with DCJTB in TPD is measured to be longer than that with DCJTB in Alq_3. These trends are opposite to those observed for rubrene-doped devices [17]. This indicates that the lifetimes of doped OLEDs are dependent primarily on the nature of the dopants and secondarily on the detailed interaction between the guest dopants and the host transport materials.

II. Experimental

Glass panels coated with 75-nm indium–tin oxide (ITO) were used as the starting substrates. The sequence of pre-cleaning prior to loading into the evaporation chamber consisted of soaking in ultra-sonic detergent for 30 min, spraying with de-ionized (DI) water for 10 min, soaking in ultra-sonic DI water for 30 min, oven bake-dry for 1–2 h and ultra-violet ozone illumination for 9 min.

A set of shadow masks was used to define the 4-mm-diameter (equivalent to an area of $\sim$12.6 mm^2) OLEDs with copper phthalocyanine (CuPc) as the anode buffer layer and TPD/Alq_3 as the active layers. The base pressure in the evaporator was $\sim 8\ \mu$ torr. The constituent organic thin films were deposited from sublimation of commercial grade CuPc, TPD and Alq_3 loaded in resistively heated evaporation cells. While the ITO formed the anodes of the OLEDs, composite layers of 0.1-nm lithium fluoride (LiF) capped with 150-nm aluminum (Al) were used as the cathodes [18]. For the doped devices, powder DCJTB was co-evaporated with TPD or Alq_3, thus giving rise to the following device configurations.

1) Doped-Alq_3 series: TPD 40 nm/Alq_3/(Alq_3 : DCJTB)/Alq_3 10 nm [Fig. 1(a)].
2) Doped-TPD series: (TPD : DCJTB)/TPD/Alq_3 50 nm [Fig. 1(b)].

Manuscript received January 25, 2001; revised June 3, 2002. This work was supported by the Hong Kong SAR Government Research Grants Council under a CRC Grant. The review of this paper was arranged by Editor J. Hynecek.

The authors are with the Center for Display Research, Department of Electrical and Electronic Engineering, The Hong Kong University of Science and Technology, Kowloon, Hong Kong (e-mail: eemwong@ee.ust.hk).

Publisher Item Identifier 10.1109/TED.2002.802620.

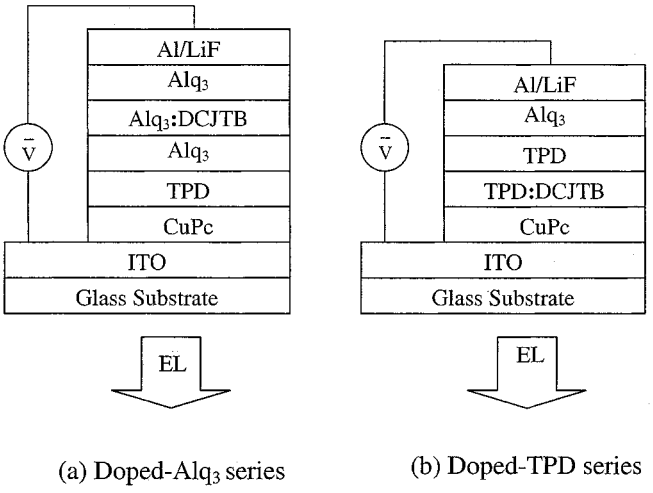

Fig. 1. Schematics of the OLED structures studied.

TABLE I
SUMMARY OF THE CONFIGURATIONS OF THE OLED DEVICES INVESTIGATED

Doped-TPD series:

ITO75nm/CuPc20nm/TPD:DCJTB/TPD/$Alq_3$50nm/LiF1nm/Al150nm

Device	TPD:DCJTB (nm)	TPD (nm)
H1	40	0
T1	25	15
T2	20	25
T3	20	35

Doped-Alq_3 series:

ITO75nm/CuPc20nm/TPD 40nm/Alq_3/Alq_3:DCJTB/$Alq_3$10nm /LiF1nm/Al150nm

Device	Alq_3 (nm)	Alq_3:DCJTB (nm)
H2	0	40
A1	10	40
A2	20	30
A3	30	20

Here, Alq_3 : DCJBT and TPD : DCJTB, respectively, indicate Alq_3 and TPD doped with DCJTB. Based on a previously reported optimization study on undoped TPD/Alq_3 OLEDs [18], respective thickness values of 20 nm, 40 nm, and 50 nm were selected for reference devices with undoped CuPc, TPD, and Alq_3. The deposition rates of the organic thin films were 0.2–0.4 nm/s. Those of LiF and Al were 0.02–0.05 nm/s and 1–1.5 nm/s, respectively. Film thickness was determined *in situ* using a crystal balance.

For the partially doped Alq_3 series, the thickness of the doped portion was varied from 20 to 40 nm. For the partially doped TPD series, the thickness of the doped portion was varied from 0 to 25 nm. The actual thickness distribution is summarized in Table I.

Devices without encapsulation were characterized in room ambient and temperature. The EL spectra and current–voltage (I–V) characteristics were measured using a Kollmorgen Instrument PR650 photospectrometer and a Hewlett-Packard HP4145B Semiconductor Analyzer, respectively. Lifetime measurements were performed in room ambient at a constant current density of 400 A/m^2.

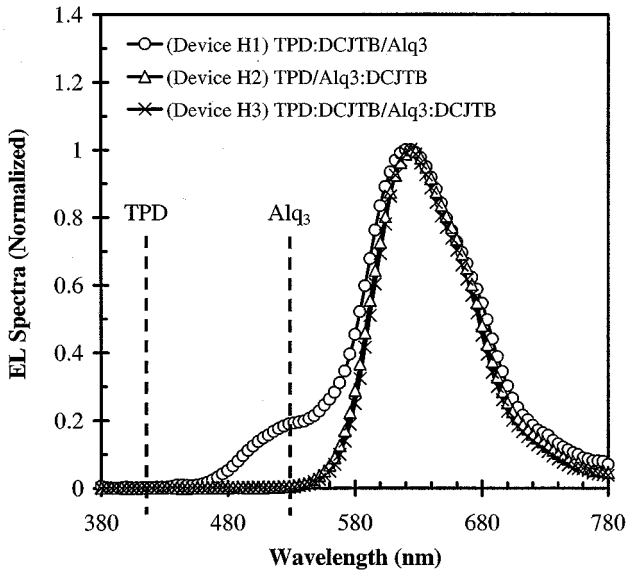

Fig. 2. EL spectra of Devices H1 (TPD : DCJTB) and H2 (Alq_3 : DCJTB).

III. RESULTS AND DISCUSSION

Host effects were studied using three kinds of devices with DCJTB incorporated at three different locations. In Devices H1 and H2, the dopant was incorporated, respectively, in TPD and Alq_3 in equal concentrations of ~5 vol%. The normalized EL spectra (Fig. 2) of the two devices are quite similar, with emission peaks located at ~620 nm. This wavelength is different from those of the reference intrinsic EL peaks of TPD and Alq_3 at ~420 nm and ~530 nm, respectively. It is attributed to the dopant molecules.

Closer inspection of the EL spectrum of Device H1 reveals a nontrivial amount of emission near the EL peak of intrinsic Alq_3 and a minute, yet still discernable, amount of emission near the EL peak of intrinsic TPD. Clearly, the conversion to dopant emission in the TPD host is slightly less efficient than that in the Alq_3 host, resulting in a) residual holes "leaking" into and initiating EL in Alq_3 and b) intrinsic TPD EL due to residual excitons in the TPD host. All such intrinsic EL can be eliminated by introducing an additional 1 vol% dopant in the Alq_3 layer in Device H3, thus giving rise to almost complete overlap (Fig. 2) of the EL spectra of Devices H2 and H3 (Fig. 2).

The luminance (L)–current–density (J)–V characteristics of Devices H1–H3, together with that of a reference intrinsic TPD/Alq_3 device, are summarized in Fig. 3. Among the four types of devices measured, the current turn-on voltage of the intrinsic device is the lowest. This is not surprising because dopant molecules give rise to traps that invariably lead to reduced charge carrier mobility [19]. A larger increase in the turn-on voltage is obtained with dopant placed in Alq_3 (Device H2) than in TPD (Device H1). This is because electron mobility in intrinsic Alq_3 is at least 100 times lower [20] than hole mobility in intrinsic TPD. Hence a much larger portion of the voltage is sustained in Alq_3. Consequently, if the dopant-induced resistance change in a host material were not excessively large, the I–V characteristics would be more sensitive to changes in the resistance of Alq_3 than those of

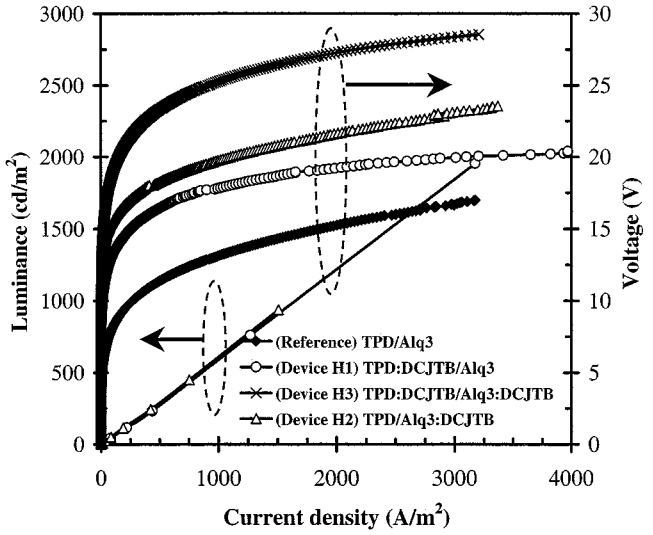

Fig. 3. The luminance (L)–current–density (J–V) characteristics of Devices H1–H3 and a reference undoped device.

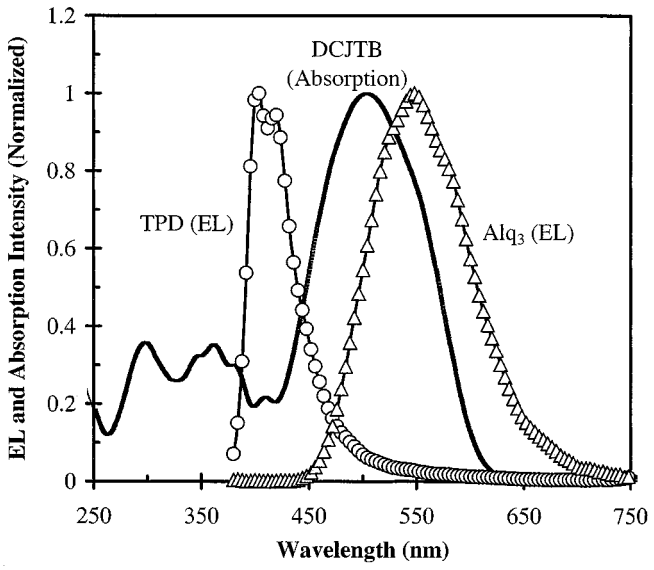

Fig. 4. Normalized spectra of TPD (EL), Alq_3 (EL), and DCJTB (Absorption).

TPD. The largest turn-on voltage is measured in Device H3, with dopant in both TPD and Alq_3.

The luminance current efficiencies (η) of the various devices can be obtained from the L–J dependence in Fig. 3. For Devices H1 and H2, η is about the same at ~0.7 cd/A (with a measured peak power efficiency of ~0.4 lm/W). Because of the different spectral response, it may be more relevant to compare the quantum efficiencies, rather than η, of Devices H1 and H2 to that of the reference device. Not surprisingly, the quantum efficiencies of the doped Devices H1 and H2 at ~5.2% are about 5× greater than that of the undoped reference device at ~1.1%.

Förster exciton transfer theory has been popularly invoked [15] to explain dopant-assisted emission in a host transport material. One characteristic parameter of the theory is the Förster radius (R_f). It is a measure of the distance over which an exciton on a host molecule can be transferred to a dopant molecule and is given by [5], [21]

$$R_f = \left[\frac{0.5291\kappa^2}{n^4 N_A}\int_0^\infty F_D(\overline{v})\varepsilon_A(\overline{v})\frac{d\overline{v}}{\overline{v}^4}\right]^{1/6}$$

where κ is a host/dopant molecule orientation factor (~0.82 for a randomly deposited film), n is the index of refraction of the host, N_A is Avogadro's number, v is the wave number, $F_D(v)$ is the normalized host emission spectrum, and $\varepsilon_A(v)$ is the dopant absorption spectrum (molar extinction coefficient). For a given dopant concentration, the larger the R_f, the more efficient is the transfer of excitons from host to dopant. The product term, $F_D(v)\varepsilon_A(v)$, inside the integral reflects the amount of the overlap between the host emission and the dopant absorption spectra. For a given host-dopant configuration, the spectra (hence, also R_f) are typically different.

The emission spectra of TPD and Alq_3, together with the absorption spectrum of DCJTB, are given in Fig. 4. Clearly the spectral overlap with DCJTB is significantly less for TPD than for Alq_3. The calculated R_f for TPD and Alq_3 are 3.4 nm and 4.3 nm, respectively. The resulting smaller R_f could have contributed to the lower efficiency of the conversion to dopant emission in the TPD-doped Device H1 than in the Alq_3-doped Device H2. However, if dopant emission in the TPD/Alq_3 system were explained using the Förster transfer theory, then the different R_f for dopants in TPD and Alq_3 would be incompatible with the almost identical η of ~0.7 cd/A measured for Devices H2 and H3.

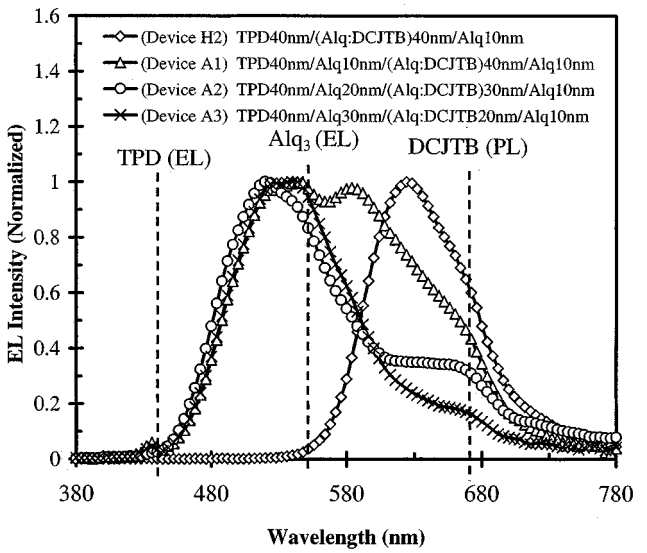

Fig. 5. EL spectra of the doped-Alq_3 series.

The equality in η could be explained if EL were dominated by sequential capture of holes and electrons in the dopant molecules, thus making the process independent of the spectra overlap shown in Fig. 4. A series of devices was fabricated to study the properties of dopants as carrier traps. Shown in Fig. 5 are the spectra of the series of doped-Alq_3 devices A1–A3. The doped Alq_3 region is separated from TPD by a layer of undoped Alq_3 with increasing thickness from Devices A1 to A3. Also shown is the spectrum of the reference Device H2, in which no undoped Alq_3 is inserted. Compared with the location of the EL peak of Device H2 at 630 nm, the insertion of 10–nm undoped Alq_3 between the doped Alq_3 and TPD in Device A1 leads to a double-peaked EL spectrum with blue-shifted peak locations

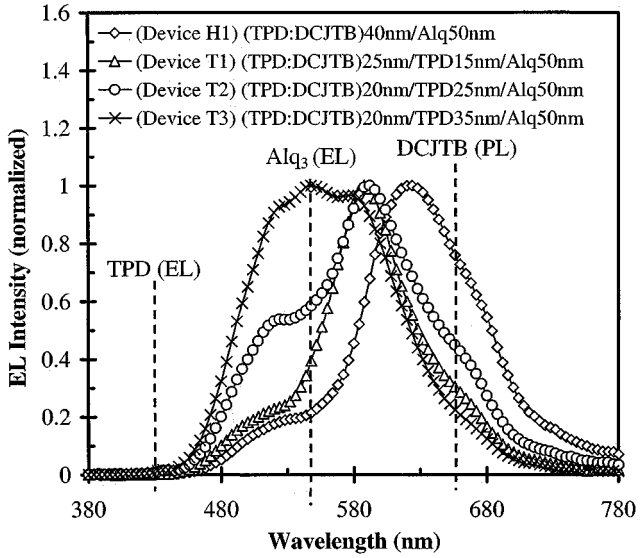

Fig. 6. EL spectra of the doped-TPD series.

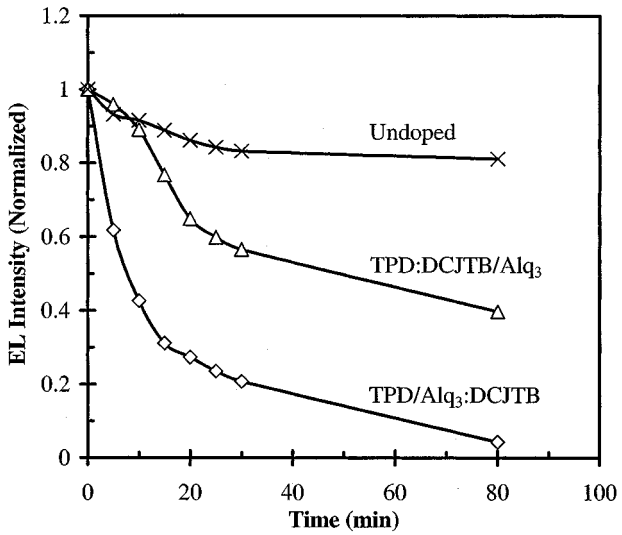

Fig. 7. Comparison of the degradation trends of Device H1 (TPD : DCJTB), Device H2 (Alq_3 : DCJTB) and a reference undoped device.

at approximately 530 nm and 580 nm. Since the 530-nm peak is quite close to the location of the EL peak of intrinsic Alq_3, it can be identified as having originated from intrinsic Alq_3 emission. It is concluded that the dopant molecules are rather weak traps of electrons. Consequently, excitons are formed largely at the interface between TPD and undoped Alq_3. Two possible mechanisms could be invoked to explain the emission at and around the longer wavelength of 580 nm: a) emission induced by the capture of diffusing excitons (Förster transfer) in the dopant molecules or b) emission resulting from dopant photo-luminescence excited by Alq_3 emission. The former mechanism is more compatible with the significant reduction in the strength of the 580 nm-peak with thicker undoped Alq_3 inserts in Devices A2 and A3, due to the finite exciton diffusion length ($\sim$20 nm) in undoped Alq_3 [22]. However, it is worth re-iterating that although Förster transfer seems to take place in doped Alq_3 already populated with excitons, it cannot be the dominant mechanism responsible for exciton formation in DCJTB when doped Alq_3 is in direct contact with the injection organic interface with TPD, given the observed equality in η of Devices H2 and H3.

Shown in Fig. 6 are the spectra of the series of doped-TPD devices T1–T3. The doped TPD region is separated from Alq_3 by a layer of undoped TPD with increasing thickness from Devices T1 to T3. In all three devices, the thickness values of the undoped TPD regions are much longer than R_f of 3.4 nm estimated for TPD. Also shown is the spectrum of the reference Device H1, in which no undoped TPD is inserted. Compared with the location of the EL peak of Device H1 at 630 nm, the insertion of 15-nm undoped TPD between the doped TPD and Alq_3 in Device T1 leads to a blue-shift of the EL peak location to approximately 580 nm, with little change in the relative EL intensity at 530 nm. Because of the hole and electron potential barriers at the TPD/Alq_3 interface, dopant emission cannot be induced by excitons diffusing into TPD from the Alq_3 side of the interface. It is concluded that the dopant molecules are stronger traps of holes. Changes in the potential distribution resulting from holes trapped in dopant molecules favor electron injection across the Alq_3/TPD barrier. The injected electrons travelling across the undoped TPD layer, when subsequently captured by the positively charged dopant molecules in the doped TPD region and recombine with the trapped holes, lead to dopant emission. Nevertheless, holes leaking through the doped TPD region are responsible for the minute amount of intrinsic TPD EL in the devices and, when injected into the Alq_3 region, for inducing emission near the intrinsic Alq_3 EL peak at 530 nm. Further increase of the undoped TPD insert to 35 nm in Device T3 resulted in a shift of the EL peak to 530 nm, though the emission spectrum still remains rather broad.

Shown in Fig. 7 are the lifetime measurements performed in room ambient at a constant J of 400 A/m^2. Roughly the same initial L values of 200 cd/m^2 and 190 cd/m^2 were obtained for the Alq_3-doped Device H1 and for the TPD-doped Device H2, respectively. It is obvious that a) the lifetimes of the doped devices are shorter than that of the reference undoped device and b) faster degradation, hence shorter lifetime, was obtained in Device H1 than in Device H2. While it is tempting to explain the shorter lifetime of Device H1 in terms of the shorter lifetime of the Alq_3 host due to the formation of reactive and unstable Alq_3 cations [23], it is unlikely that this would be a general explanation applicable to all dopants. In fact, the trends are completely opposite in rubrene-doped systems [17], the lifetimes of which are found to be 1) longer than those of the undoped devices and 2) shorter with dopant in the HTL than those with dopant in the ETL. Therefore, while it is clear that lifetimes are intrinsically controlled by the stability of the dopant molecules, the host effects can be rather subtle and depend on the detailed interactions between the dopant and the host materials.

IV. Conclusion

A series of devices with the dopant DCJTB placed in different regions of TPD, HTL, and Alq_3 ETL has been studied. It is proposed that sequential carrier trapping, rather than Förster transfer, is the more likely mechanism of dopant emission for dopant molecules located immediately adjacent to the organic

interface. Studies of the lifetimes of various device configurations reveal that lifetimes are intrinsically controlled by the stability of the dopant molecules, but the host effects can be rather subtle and depend on the detailed interactions between the dopant and the host materials.

REFERENCES

[1] P. E. Burrows, G. Gu, V. Bulovic, Z. Shen, S. R. Forrest, and M. E. Thompson, "Achieving full-color lightweight, flat-panel displays," *IEEE Trans. Electron Devices*, vol. 44, pp. 1188–1202, Aug. 1997.

[2] Y. Kijima, N. Asai, and S. Tamura, "A blue organic light emitting diode," *Jpn. J. Appl. Phys.*, vol. 38, pp. 5274–5277, 1999.

[3] R. H. Jordan, A. Dodabalapur, M. Strukelj, and T. M. Miller, "White organic electroluminescence devices," *Appl. Phys. Lett.*, vol. 68, no. 9, pp. 1192–1194, 1996.

[4] C. W. Tang and S. A. Van Styke, "Organic electroluminescent diode," *Appl. Phys. Lett.*, vol. 51, pp. 913–915, 1987.

[5] A. A. Shoustikov, Y. You, and M. E. Thompson, "Electroluminescence color tuning by dye doping in organic light-emitting diodes," *IEEE J. Select. Topics Quantum Electron.*, vol. 4, pp. 3–13, Jan. 1998.

[6] X. T. Tao, S. Miyata, H. Sasabe, G. J. Zhang, T. Wada, and M. H. Jiang, "Efficient organic red electroluminescent device with narrow emission peak," *Appl. Phys. Lett.*, vol. 78, no. 3, pp. 279–281, 2001.

[7] M. Mitsuya, T. Suzuki, T. Koyama, H. Shirai, and Y. Taniguchi, "Bright red organic light-emitting diodes doped with a fluorescent dye," *Appl. Phys. Lett.*, vol. 77, no. 20, pp. 3272–3274, 2000.

[8] H. Murata, C. D. Merritt, and Z. H. Kafafi, "Emission mechanism in rubrene-doped molecular organic light-emitting diode direct carrier recombination at luminescent centers," *IEEE J. Select. Topics Quantum Electron.*, vol. 4, no. 1, pp. 119–124, 1998.

[9] H. Heil, J. Steiger, R. Schmechel, and H. von Seggern, "Tris(dibenzoylmethane) (monophenanthroline)europium(III) based red emitting organic light emitting diodes," *J. Appl. Phys.*, vol. 90, no. 10, pp. 5357–5362, 2001.

[10] Y. Hamada, T. Sano, K. Shibata, and K. Kuroki, "Influence of the emission site on the running durability of organic electroluminscent devices," *Jpn. J. Appl. Phys. (Part 2) Lett.*, vol. 34, pp. L824–828, 1995.

[11] H. Vestweber and W. Riess, "Highly efficient and stable organic light-emitting diodes," *Synthetic Metals*, vol. 91, no. 1–3, pp. 181–185, 1997.

[12] Y. Sato, S. Ichinosawa, and H. Kanai, "Operation characteristics and degradation of organic electroluminescent devices," *IEEE J. Select. Topics Quantum Electron.*, vol. 4, no. 1, pp. 40–48, 1998.

[13] J. Shi and C. W. Tang, "Doped organic electroluminescent devices with improved stability," *Appl. Phys. Lett.*, vol. 70, pp. 1665–1667, 1997.

[14] S. A. Van Slyke, C. H. Chen, and C. W. Tang, "Organic electroluminescent devices with improved stability," *Appl. Phys. Lett.*, vol. 69, pp. 2160–2162, 1996.

[15] V. G. Kozlov, V. Bulovic, P. E. Burrows, M. Baldo, V. B. Khalin, G. Parthasarathy, S. R. Forrest, Y. You, and M. E. Thompson, "Study of lasing action based on Förster energy transfer in optically pumped organic semiconductor thin films," *J. Appl. Phys.*, vol. 84, no. 8, pp. 4096–4108, 1998.

[16] H. Murata, C. D. Merritt, and Z. H. Kafafi, "Emission mechanism in rubrene-doped molecular organic light-emitting diodes: Direct carrier recombination at luminescent centers," *IEEE J. Select. Topics Quantum Electron.*, vol. 4, no. 1, pp. 119–124, 1998.

[17] G. Sakamoto, C. Adachi, T. Koyama, and Y. Taniguchi, "Significant improvement of device durability in organic light-emitting diodes by doping both hole transport and emitter layers with rubrene molecules," *Appl. Phys. Lett.*, vol. 75, no. 6, pp. 766–768, 1999.

[18] C. Qiu, H. Chen, M. Wong, and H. S. Kwok, "Dependence of the current and power efficiencies of organic light-emitting diode on the thickness of the constituent organic layers," *IEEE Trans. Electron Devices*, vol. 48, pp. 2131–2137, Sept. 2001.

[19] N. von Malm, J. Steiger, R. Schmechel, and H. von Seggern, "Trap engineering in organic hole transport materials," *J. Appl. Phys.*, vol. 89, no. 10, pp. 5559–5563, 2001.

[20] S. Barth, P. Mueller, H. Riel, P. F. Seidler, and W. Riess, "Electron mobility in tris(8-hydroxy-quinoline)aluminum thin films determined via transient electroluminescence from single- and multilayer organic light-emitting diodes," *J. Appl. Phys.*, vol. 89, no. 7, pp. 3711–3719, 2001.

[21] K. Read, H. S. Karlsson, M. M. Murnane, H. C. Kapteyn, and R. Haight, "Excitation dynamics of dye doped tris (8-hydroxyquinoline) aluminum films studied using time-resolved photoelectron spectroscopy," *J. Appl. Phys.*, vol. 90, no. 1, pp. 294–300, 2001.

[22] C. W. Tang, S. A. Van Slyke, and C. H. Chen, "Electroluminescence of doped organic thin film," *J. Appl. Phys.*, vol. 65, no. 9, pp. 3610–3616, 1989.

[23] H. Aziz, Z. D. P., N.-X. Hu, A.-M. Hor, and G. Xu, "Degradation mechanism of small molecule-based organic light-emitting devices," *Science 283*, vol. 19, pp. 1900–1902, Mar. 1999.

Chengfeng Qiu received the B.S. degree in physics from Nankai University, Tianjin, China, in 1982, and the Ph.D. degree in material science from Xian Jiaotong University, Xian, China, in 1993.

From 1982 to 1993, he was with the Electronic Engineering Department, Xian Jiaotong University, doing research on the modification of material surfaces using ion beam treatment, ion implantation, and thin-film deposition. From 1993 to 1995, he was with Tianma Microelectronics, China, and worked on liquid-crystal displays. From 1995 to 2000, he was with STD, China, and was the Vice-President responsible for the research, development, and manufacturing of liquid-crystal display products. Currently, he is a Postdoctoral Fellow at the Center for Display Research, Hong Kong University of Science and Technology, Hong Kong, doing research on organic light-emitting diodes.

Haiying Chen received the B.S. and M.S. degrees in engineering and material science and engineering from Tsinghua University, Beijing, China, in 1996 and 1999, respectively. She is currently pursuing the Ph.D. degree in the Department of Electrical and Electronic Engineering, Hong Kong University of Science and Technology, Hong Kong.

Man Wong (SM'00) was born in Beijing, China. He attended primary and secondary schools in Hong Kong. He received the B.S. and M.S. degrees in electrical engineering from the Massachusetts Institute of Technology, Cambridge, and the Ph.D. degree in electrical engineering from Stanford University, Stanford, CA.

From 1985 to 1988, he was with the Center for Integrated Systems, Stanford University, where he worked on tungsten gate MOS technology. He then joined the Semiconductor Process and Design Center of Texas Instruments, Dallas, TX, and worked on the modeling and development of IC metallization systems and dry/vapor cleaning processes. In 1992, he joined the Faculty of the Department of Electrical and Electronic Engineering, Hong Kong University of Science and Technology, Hong Kong. His current research interests include microfabrication technology, device structure and material, thin-film transistors, organic light-emitting diodes, display technology, and integrated microsystems.

Dr. Wong is a member of Tau Beta Pi, Eta Kappa Nu, and Sigma Xi.

Hoi S. Kwok received the Ph.D. degree in applied physics from Harvard University, Cambridge, MA, in 1978.

He joined the State University of New York, Buffalo, in 1980 as an Assistant Professor in the Department of Electrical and Computer Engineering, and was promoted to the rank of full Professor in 1985. He joined the Hong Kong University of Science and Technology, Hong Kong, in December 1992 and is currently Director of the Center for Display Research. He has more than 250 refereed publications and holds more than ten patents in optics and LCD technologies.

Dr. Kwok was awarded the U.S. Presidential Young Investigator Award in 1984 and is a Fellow of the Optical Society of America. He is currently Chairman of the Society of Information Display, Hong Kong Chapter.